Appl. Phys. A 88, 341–345 (2007)
DOI: 10.1007/s00339-007-3938-4

Applied Physics A
Materials Science & Processing

J.C. HAN
A.P. LIU✉
J.Q. ZHU
M.L. TAN
H.P. WU

Effect of phosphorus content on structural properties of phosphorus incorporated tetrahedral amorphous carbon films

Center for Composite Materials, Harbin Institute of Technology, Post-Box 3010, Yikuang Street 2, Nangang District, Harbin 150080, P.R. China

Received: 18 October 2006/Accepted: 5 February 2007
Published online: 22 March 2007 • © Springer-Verlag 2007

ABSTRACT With phosphorus incorporated tetrahedral amorphous carbon (ta-C:P) films prepared using filtered cathodic vacuum arc technique with PH_3 as the dopant source, we investigate the effect of phosphorus content on the structural properties of the films by X-ray photoelectron spectroscopy (XPS) and Raman spectroscopy. XPS analysis indicates that a function is established between the atomic fraction of phosphorus in the samples and the flow rate of PH_3 during deposition, and that phosphorus implantation increases the graphite-like trihedral sp^2 bonds deduced from fitted C 1*s* and P 2*p* core level spectra. Raman spectra of a broad range show that there are two notable features for all ta-C:P films: the first-order band centered at about 1560 cm^{-1} and the second-order band between 2400 and 3400 cm^{-1}. The broad first-order band demonstrates that the amorphous structure of all samples does not remarkably change when a lower flow rate of PH_3 is implanted, while a higher concentration of phosphorus impurity enhances the clustering of sp^2 sites dispersed in sp^3 skeleton and the evolution of structural ordering. Furthermore, the second-order Raman spectra confirm the formation of small graphitic crystallites in size due to a finite-crystal-size effect.

PACS 81.05.Uw; 81.15.Ef; 63.50.+x

1 Introduction

The research on tetrahedral amorphous carbon (ta-C) films has attracted much attention for its excellent properties, such as high hardness, low wear, good biological compatibility, and so on. There has been recently enlarged interest in its application as an electronic material. Boron is a common dopant used in carbon films to form a *p*-type conductive semiconductor [1, 2]. Most of the previous examinations have concentrated on nitrogen as an *n*-type dopant because of its size similar to carbon [3–5]. For the same reason, phosphorus is widely used in silicon [6] and diamond [7, 8] to achieve *n*-type doping. But not much attention is paid to the influence of the addition of P on amorphous carbon (a-C).

There have been various deposition methods and attempted dopant sources for the preparation of phosphorus incorporated a-C films (a-C:P). For example, McKenzie et al. adopted a red phosphorus-doped graphite cathode to produce ta-C:P films using a filtered cathodic vacuum arc (FCVA) method [9]. With camphor used as a natural carbon precursor, Krishna deposited an *n*-type a-C:P films via pyrolysis and ion-beam sputtering [10]. Pulsed-laser methods were also used to synthesize diamond-like carbon films with various phosphorus fractions [11–13]. Besides red phosphorus, trimethylphosphite ($P(OCH_3)_3$) and phosphine (PH_3) were employed as the doping sources [14–16]. These a-C:P films exhibit many outstanding properties and can be applied in the fields of photovoltaic solar cell [10, 17, 18] and semiconductor field emitter [14]. However, insufficient work has been done on the structural properties of a-C:P films which have significant effect on their performance and applications. It is generally accepted that X-ray photoemission spectroscopy (XPS) is a powerful tool used to characterize the local environment and investigate the local binding properties of materials in a given system. Unfortunately, the unknown local environments and the lack of references make it difficult to interpret the contributions of C 1*s* and P 2*p* core level spectra to a-C:P films [13, 16, 19]. Additionally, Raman spectroscopy is one of the most sensitive methods and important techniques used to distinguish ordered and disordered carbon materials. The Raman analysis of a-C:P films has been reported in some of the previous work [11, 13, 14, 16, 20]. However, most of them focus on the first-order band ranging from 800 to 2000 cm^{-1} and no attention has been given on the second-order band ranging from 2400 to 3400 cm^{-1}. Considering the graphitization tendency can be deduced from the variation of the first-order band in the shape and size and the second-order band is regarded as the scale of crystallinity changes [21], it is necessary to examine the properties of films by Raman spectroscopy in a wider range.

In this paper a new technology is proposed for preparing ta-C:P films using FCVA. PH_3 is widely used in the semiconductor industry to introduce phosphorus into silicon crystals as an intentional impurity [6, 22]. May et al. also synthesized a-C:P film with CH_4 and PH_3 mixtures as the process gases [15, 23]. So PH_3 is a good dopant to prepare ta-C:P(H) films. The effect of phosphorus content on the structural properties of the films is analysed in detail by XPS and Raman spectroscopy.

✉ Fax: +86-451-86417970, E-mail: liuaiping1979@gmail.com

2 Experimental details

Ta-C and ta-C:P films were synthesized on p-type silicon wafers by FCVA system which has been described elsewhere [24]. Prior to deposition the vacuum chamber was pumped down to 2×10^{-6} Torr and a 80-V negative bias was added to the substrate. Argon ions were used to etch the substrates for approximately 5 min. The arc was then ignited by contacting the graphite anode against the graphite cathode (purity 99.999%). In order to introduce the impurity, PH_3 was implanted into the vacuum chamber via a gas source. The partial pressure of PH_3 varied from 2.4×10^{-5} to 2.7×10^{-4} Torr as the PH_3 flow rate increased from 3 to 30 sccm. The thickness of all samples determined by spectroscopic ellipsometry was 40–50 nm.

XPS analysis was made using a PHI ESCA 5700 spectrometer with Al K_α (1486.6 eV) as the X-ray soure. XPS core level spectra scan for C 1s, P 2p and O 1s was done at 0.125 eV step with a pass energy of 30 eV. XPS spectra were also recorded after the film surface was sputtered with 3 kV argon ions for two minutes. The compositions of the films were analyzed and quantified for phosphorus, carbon and oxygen elements from the total areas of XPS signals corresponding to P 2p, C 1s and O 1s spectra using the sensitivity factors of the instrument. Raman analysis was performed on a Jobin Yvon Labram HR 800 spectrometer with 458 nm lines of an Ar^+ excitation source. Laser power was 20 mW, and typical data acquisition time was 100 s. The recorded wave length ranged from 600 to 3500 cm^{-1}.

3 Results and discussion

3.1 *XPS analysis*

Figure 1 shows a typical XPS overview of ta-C and ta-C:P films. The existence of P in the film is indicated by the two peaks located at 132.4 ± 0.2 eV and 189.5 ± 0.2 eV as P 2p and P 2s spectra, respectively. The peak centered at 285.4 ± 0.2 eV is caused by the photoelectrons excited from the C 1s spectra. A slight shift of C 1s spectrum towards a lower binding energy is detected by the addition of phosphorus. An oxygen signal at 533.2 ± 0.2 eV is the result of air exposure during the experiment and sample transport. The content of phosphorus over the sum of phosphorus and carbon (P/(C + P)) is calculated and recorded from 0 to 16.83 at. % as the flow rate of PH_3 increases from 0 to 30 sccm. Figure 2 shows the relationship between the ratio of P and C atoms, P:C, and the flow rate of PH_3 during deposition with an error of less than 5%.

Figure 3 displays the evolution of C 1s and P 2p spectra. A small but significant variation of peak maxima and the full width at half maximum (FWHM) of C 1s peaks indicates the changes in binding states of ta-C:P films. For lack of unequivocal evidence for the contribution of C and P bonds in the films, we assume for following discussion that ta-C:P films contain little C−P bonding or the contribution of C−P bonds is ignored as Claeyssens et al. did [16, 19]. C 1s spectra are then fitted with three lines for all films using a combination of 80% Gaussian and 20% Lorentzian function [25] as shown in Fig. 3a–c. The C1 and C2 peaks established at 284.5 ± 0.2 eV and 285.5 ± 0.2 eV correspond to sp^2- and sp^3-hybridized C−C bonds, respectively [26]. The third peak (C3) at 287 ± 0.2 eV accounts for a C−O or C=O contribution due to air exposure [27]. The content of each hybrid carbon is, therefore, determined as the ratio of corresponding peak area over total C 1s peak area. The calculation indicates that the percentage of sp^3-hybrided carbon declines with the increase of phosphorus concentration in ta-C:P films. The sp^3/sp^2 ratio drops from 6.04 to 2.34 with the P:C ratio up to 0.202. The similar tendency can be deduced from [19]. It can, therefore, be concluded that phosphorus impurity enhances the graphite-like trihedral sp^2 bonds in films.

As shown in Fig. 3d–f, due to the non-symmetric line shape the experimental P 2p spectra are fitted with a combination of two contributions: a low binding energy component centered at 131.3 ± 0.2 eV (P1) and a high binding energy component centered at 133.4 ± 0.2 eV (P2), respectively. Considering the assumption of negligible C−P bonds above, we assign the low binding energy component to the possible function of P−P or P−H feature [19, 28], while the high energy component is associated with P−O bonding [19, 28]. It should

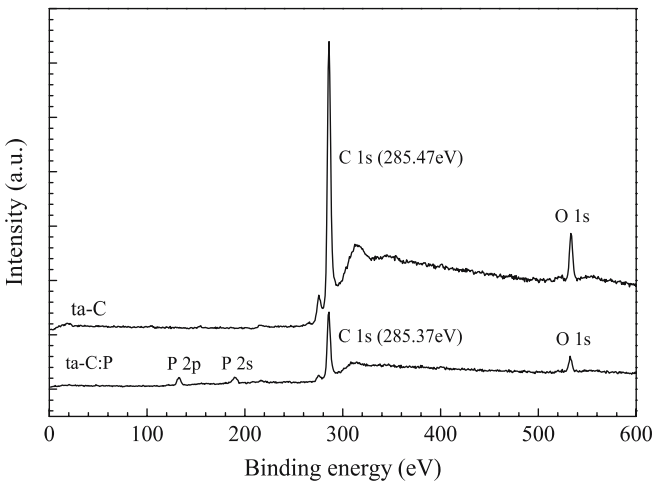

FIGURE 1 XPS spectra of ta-C and ta-C:P film with 10-sccm PH_3 introduced

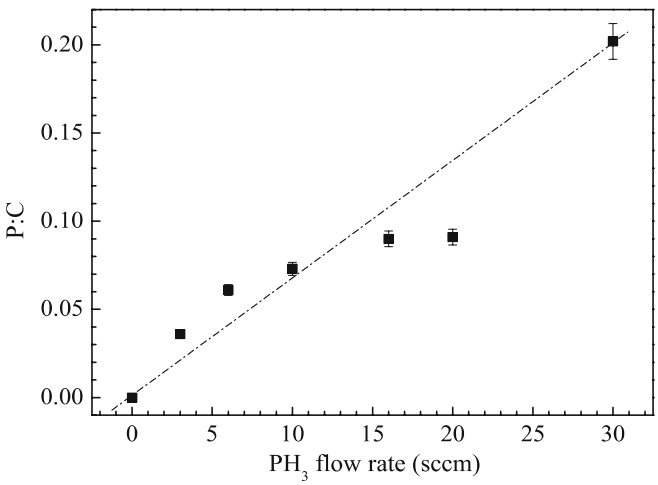

FIGURE 2 Relationship between the ratio of P and C atomic content, P:C, in ta-C:P films and flow rate of PH_3 during deposition

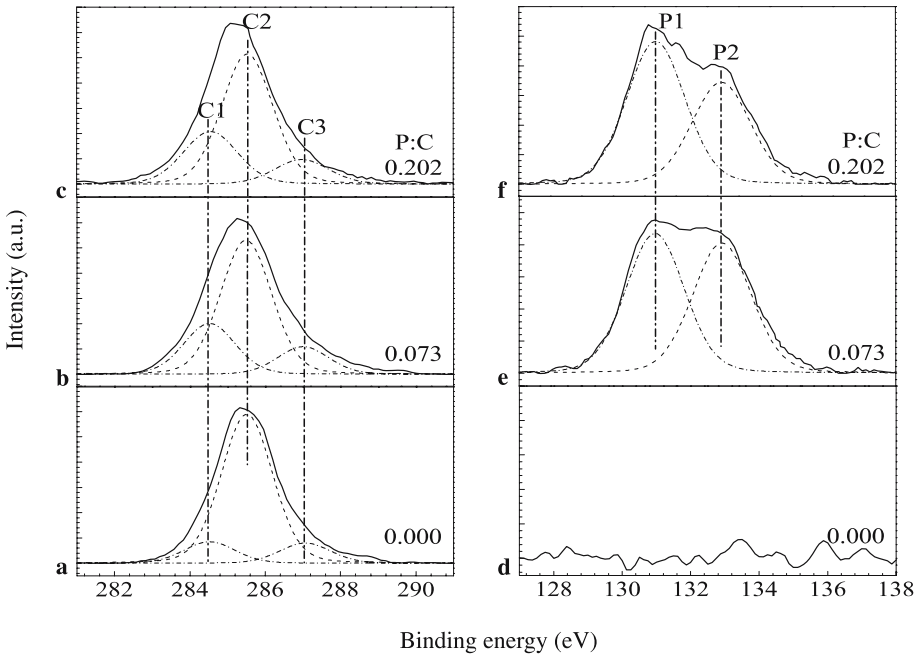

FIGURE 3 XPS core level spectra as a function of P:C ratio in carbon films, (**a**)–(**c**) are C 1*s* lines; (**d**)–(**f**) are P 2*p* lines. *Solid lines* and *dash lines* are measured and fitted peaks, respectively. Three peaks (C1, C2 and C3) in C 1*s* spectra contribute to C-sp^2 (centered at 284.5 eV), C-sp^3 (centered at 285.5 eV) and C−O bonds (centered at 287 eV); two peaks (P1 and P2) in P 2*p* spectra contribute to PP/PH and P−O binding

be noted that XPS analysis of C 1*s* and P 2*p* spectra is qualitative based on the reasonable assumption for lack of any evidence for the existence and forms of P and C bonding in ta-C:P films, and so further theoretical and experimental exploration should be performed to reveal the interactions between P and C atoms.

3.2 *Raman analysis*

It can be seen from Raman spectra of ta-C and ta-C:P films with different P:C ratio shown in Fig. 4 that there are three obvious features, the first-order peak of carbon between 1000 and 1800 cm^{-1}, the second-order peak of carbon between 2400 and 3400 cm^{-1} [29] and the second-order peak of silicon centered at about 980 ± 2 cm^{-1}. No peak associated with phosphorus is observed in Raman spectra for any of the samples. Considering the asymmetry of first-order band, we find that it depends on D peak centered at about 1380 ± 5 cm^{-1} and G peak centered at 1560 ± 10 cm^{-1}. G peak is attributed to the bond stretching of all pairs of sp^2 atoms in rings as well as chains, while D peak is the breathing modes of disordered graphite rings. No evident "peak shoulder" of D peak is detected until the P:C ratio rises up to 0.202, which suggests the increasing ordered aromatic rings.

As shown in Fig. 5, a standard fitting procedure is employed for the first-order band by using two Gaussian lines with the linear background subtracted, and such parameters as peak positions, FWHM and intensity ratio of peaks (I_D/I_G) are obtained by fitting with the allowable error of 5%. A downshift of G-peak position is detected with the flow rate of PH_3 elevation except for an abnormal site with 30-sccm PH_3 implanted, while the variation of D-peak position is negligible. It can be seen from Fig. 6 that a mild increase of the I_D/I_G ratio

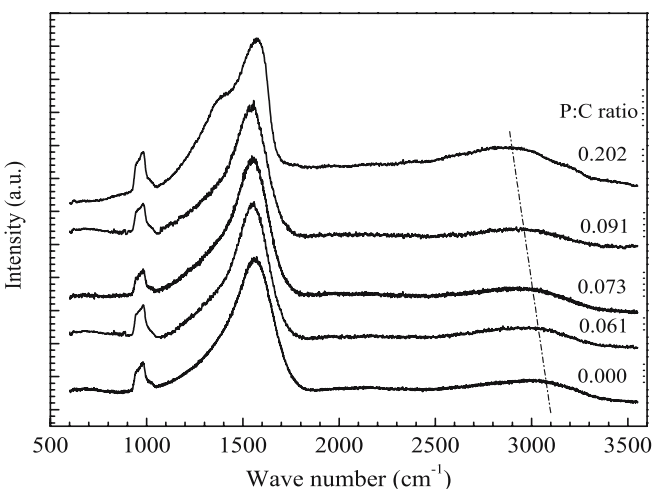

FIGURE 4 Raman spectra of ta-C and ta-C:P films with various P:C ratio in films

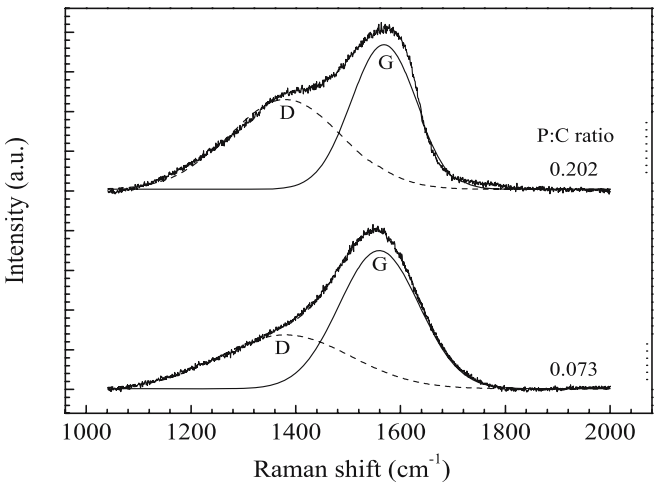

FIGURE 5 Raman spectra of ta-C:P films with P:C ratio of 0.073 and 0.202 deconvolved with two Gaussian line-shape functions. *Broad lines* are the measurements; *dash lines* and *thin solid lines* are fitted D and G peaks

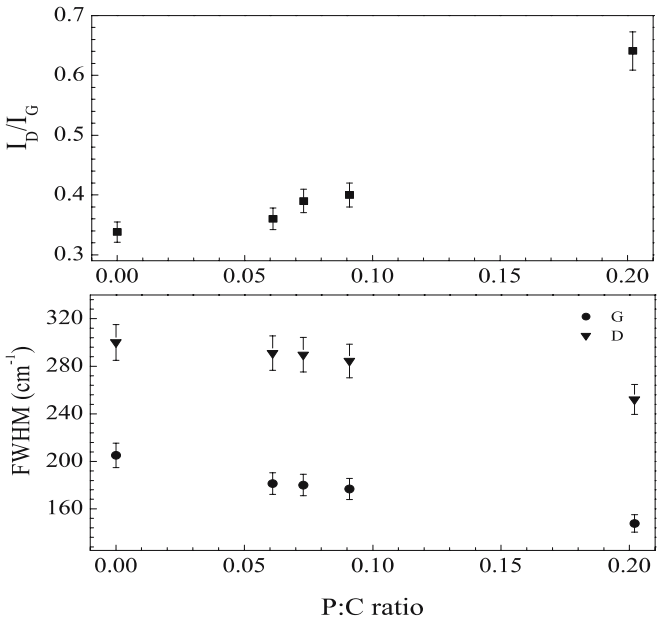

FIGURE 6 I_D/I_G ratio and FWHM of D peak and G peak as a function of P:C ratio

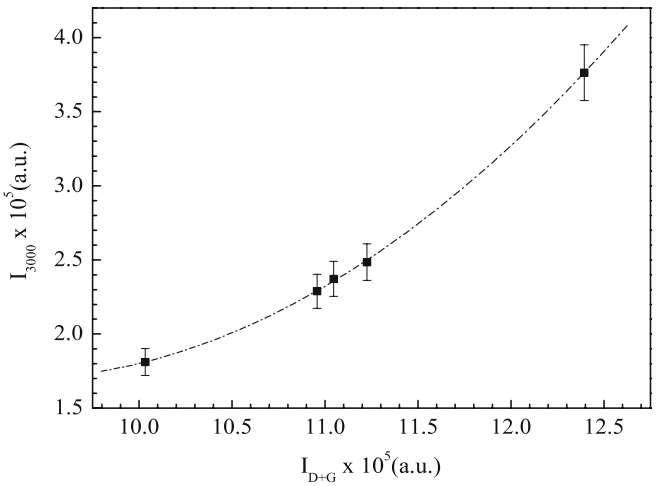

FIGURE 7 Relationship between integrated intensity of second-order band, I_{3000}, and sum integrate intensity of D and G peaks, I_{D+G}, for ta-C:P films with various phosphorus content

from 0.34 to 0.4 is observed with P:C radio up to 0.091, while the trend becomes steeper at a higher P:C ratio of 0.202. The tendency of the D-peak and G-peak width upon P:C ratio is just inverse. We can, therefore, infer that the enhancement of I_D/I_G ratio and the reduction of FWHM of G peak characterize a clustering process of isolated sp^2 pairs distributed in the sp^3 skeleton of the films. A tendency towards graphitization is introduced by the growing phosphorus content, accompanied by an increasing level of structural ordering, and this is full in line with the results of Claeyssens et al. [19].

The second-order Raman effect involves the actions of two phonons [30]. One of the most successful applications in the second-order Raman scattering is the examination of diamond [31, 32] and amorphous carbon nitride films [33, 34] though there is still another understanding of CH stretching vibration modes [35]. The broad band between 2400 and 3400 cm^{-1} is proved in the present work to be the second-order spectra for following two points: (a) the band is located in ta-C film without hydrogen; (b) the band can be clearly seen when ta-C:P films are annealed at 700 °C at which hydrogen comes out from the films. Because its evident asymmetry, the broad second-order band is fitted using three Gaussian lines in the way of Messina et al. [33], i.e., three bands centered at the approximate frequency positions for 2ωD (the frequency of D peak), 2ωG (the frequency of G peak), and the combination of ωD and ωG [36]. It can be seen from Fig. 4 that there is a downshift of second-order-peak center from 3021 ± 3 to 2907 ± 3 cm^{-1} because of enhancing role of the peak at 2ωD. Moreover, the second-order spectrum exhibits an interesting dependence on crystallite size [21, 29]. The spectrum broadens consistently with the increase of graphitic crystallites in size. The relationship between the integrated intensity of the second-order band, I_{3000}, and the sum integrated intensity of D and G peaks, I_{D+G}, for ta-C:P films with various phosphorus content is as shown in Fig. 7. The quadratic mode obtained is just like that of Messina et al. [33].

It should be noted that the photoluminescence (PL) background can be seen from Raman spectra when flow rate of PH_3 up to 30 sccm. Similar to a-C:H films, the PL comes from isolated sp^2 clusters, and its intensity increases with the H content due to the progressive saturation of carbon dangling bonds [37]. The main influence of H in ta-C:P(H) films is to modify the carbon network by H saturating C=C bonds as $=CH_x$ groups, rather than by increasing the fraction of C−C bonds [38]. But even if the CH_x groups do exist, the broad band centered at about 3000 cm^{-1} is the feature of second-order Raman band representing sp^2-bonded-carbon vibration behavior. When the ta-C:P(H) film is annealed at 700 °C even higher the band can be distinctly detected from the hydrogen evolution in the film [39, 40]. The relationship between I_{3000} and I_{D+G} at various annealing temperature is also in agreement with the quadratic mode. Wang's research confirmed the second-order band feature by annealing a-C:H films at 1000 °C [41]. Thus, the contribution of CH bonds is slight and negligible for the analysis of Raman spectra.

4 Conclusions

Phosphorus incorporated tetrahedral amorphous carbon films are deposited using filtered cathodic vacuum arc technique with PH_3 as dopant and characterized by XPS and broad-range Raman spectra. The atomic fraction of phosphorus in the films increases with the enhancement of PH_3 flow rate, which results in the transformations of local carbon hybridization states from sp^3 to sp^2. A lower phosphorus content does not prominently agitate the amorphous structures of the films, but a higher-concentration phosphorus accelerates the clustering of sp^2 sites and the ordered level of the structure, representing the notable increase of I_D/I_G ratio and the decline of FWHM of G peak in the first-order Raman band. Furthermore, the broadening second-order Raman spectra validate the existence of small graphitic crystallites based on a finite-crystal-size effect. The quadratic mode relationship between the integrated intensity of second-order and first-order band is established for the films with various phosphorus content.

ACKNOWLEDGEMENTS We would like to thank the National Natural Science Foundation of China (Grant No. 50602012) for its financial support and Dr. Sun Mingren and Miss. Chen Yajie for their assistance provided in doing XPS experiment and Raman spectra measurements.

REFERENCES

1 N. Konofaos, C.B. Thomas, J. Appl. Phys. **81**, 6238 (1997)
2 C.H. Lee, K.S. Lim, Appl. Phys. Lett. **72**, 106 (1998)
3 R. Kalish, O. Amir, R. Brener, R.A. Spits, T.E. Derry, Appl. Phys. A **52**, 48 (1991)
4 J. Robertson, C.A. Davis, Diam. Relat. Mater. **4**, 441 (1995)
5 B.S. Satyanarayana, A. Hart, W.I. Milne, J. Robertson, Appl. Phys. Lett. **71**, 1430 (1997)
6 M.P. Petkov, M.H. Weber, K.G. Lynn, R.S. Crandall, V.J. Ghosh, Phys. Rev. Lett. **82**, 3819 (1999)
7 N.D. Samsonenko, V.V. Tokiy, S.V. Gorban, V.I. Timchenko, Surf. Coat. Technol. **47**, 618 (1991)
8 S. Koizumi, K. Watanabe, F. Hasegawa, H. Kanda, Science **292**, 1899 (2001)
9 V.S. Veerasamy, G.A.J. Amaratunga, C.A. Davis, A.E. Timbs, W.I. Milne, D.R. McKenzie, J. Phys.: Condens. Matter **5**, L169 (1993)
10 K.M. Krishna, M. Umeno, Y. Nukaya, T. Soga, T. Jimbo, Appl. Phys. Lett. **77**, 1472 (2000)
11 S.M. Mominuzzaman, T. Soga, T. Jimbo, M. Umeno, Diam. Relat. Mater. **10**, 1839 (2001)
12 M. Rusop, T. Soga, I. Jimbo, Diam. Relat. Mater. **13**, 2197 (2004)
13 G.M. Fuge, P.W. May, K.N. Rosser, S.R.J. Pearce, M.N.R. Ashfold, Diam. Relat. Mater. **13**, 1442 (2004)
14 C.L. Tsai, C.F. Chen, C.L. Lin, J. Appl. Phys. **90**, 4847 (2001)
15 M.T. Kuo, P.W. May, A. Gunn, M.N.R. Ashfold, R.K. Wild, Diam. Relat. Mater. **9**, 1222 (2000)
16 F. Claeyssens, G.M. Fuge, N.L. Allan, P.W. May, S.R.J. Pearce, M.N.R. Ashfold, Appl. Phys. A **79**, 1237 (2004)
17 K.M. Krishna, T. Soga, T. Jimbo, M. Umeno, Carbon **37**, 531 (1999)
18 M. Rusop, T. Soga, T. Jimbo, Sol. Energ. Mater. Sol. Cells **90**, 291 (2006)
19 F. Claeyssens, G.M. Fuge, N.L. Allan, P.W. May, M.N.R. Ashfold, Dalton Trans. **19**, 3085 (2004)
20 M. Rusop, H. Ebisu, M. Adachi, T. Soga, T. Jim, Japan. J. Appl. Phys. **44**, 6124 (2005)
21 Y.J. Lee, J. Nucl. Mater. **325**, 174 (2004)
22 K. Kadas, G.G. Ferenczy, S. Kugler, J. Non-Cryst. Solids **227**, 367 (1998)
23 S.R.J. Pearce, P.W. May, R.K. Wild, K.R. Hallam, P.J. Heard, Diam. Relat. Mater. **11**, 1041 (2002)
24 J.Q. Zhu, J.C. Han, X. Han, S.H. Meng, A.P. Liu, X.D. He, Opt. Mater. **28**, 473 (2006)
25 G. Beamson, D. Briggs, *High Resolution XPS of Organic Ploymer – The Scienta ESCA300 Database* (Wiley, UK, 1992)
26 T.Y. Leung, W.F. Man, P.K. Lim, W.C. Chan, F. Gaspari, J. Non-Cryst. Solids **254**, 156 (1999)
27 T.Y. Leung, MPhil thesis (Department of Physics, Hong Kong Baptist University, 1998)
28 J.F. Moulder, W.F. Stickle, *Handbook of X-Ray Photoelectron Spectroscopy* (Perkin-Elmer Corporation, Eden Prairie, MN, USA, 1979)
29 R.J. Nemanich, S.A. Solin, Phys. Rev. B **20**, 392 (1979)
30 R. Loudon, Adv. Phys. **50**, 813 (2001)
31 E.H. Lee, D.M. Hembree Jr., G.R. Rao, L.K. Mansur, Phys. Rev. B **48**, 15 540 (1993)
32 H. Herchen, M.A. Cappelli, Phys. Rev. B **49**, 3213 (1994)
33 G. Messina, A. Paoletti, S. Santangelo, A. Tagliaferro, A. Tucciarone, J. Appl. Phys. **89**, 1053 (2001)
34 M. Tabbal, T. Christidis, S. Isber, P. Merel, M.A. El Khakani, M. Chaker, A. Amassian, L. Martinu, J. Appl. Phys. **98**, 044 310 (2005)
35 M.K. Fung, W.C. Chan, Z.Q. Gao, I. Bello, C.S. Lee, S.T. Lee, Diam. Relat. Mater. **8**, 472 (1999)
36 R.B. Wright, R. Varma, D.M. Gruen, J. Nucl. Mater. **63**, 415 (1976)
37 B. Marchon, J. Gui, K. Grannen, G.C. Rauch, J.W. Ager, S.R.P. Silva, J. Robertson, IEEE Trans. Magn. **33**, 3148 (1997)
38 C.S. Lee, J.K. Shin, K.Y. Eun, K.R. Lee, K.H. Yoon, J. Appl. Phys. **95**, 4829 (2004)
39 R. Stief, J. Schafer, J. Ristein, L. Ley, J. Non-Cryst. Solids **198**, 636 (1996)
40 N.M.J. Conway, A.C. Ferrari, A.J. Flewitt, J. Robertson, W.I. Milne, A. Tagliaferro, W. Beyer, Diam. Relat. Mater. **9**, 765 (2000)
41 Q. Wang, D.D. Allred, J. Gonzalez-Hernandez, Phys. Rev. B **47**, 6119 (1993)